International Journal of Nanoelectronics and Materials
IJNeaM
ISSN 1985-5761 | E-ISSN 2232-1535

Optimizing $BaTiO_3$ Content in Flexible PVDF Films for Enhanced Piezoelectric Nanogenerator Performance

Habibah Zulkefle[a,*], Muhammad Izz Danial Mohd Muzaini[a], Norhafizah Burham[a], Dayana Kamaruzaman[b], Nor Diyana Md Sin[c], Nurfadzilah Ahmad[a], Puteri Sarah Mohamad Saad[a], and Firdaus Muhammad-Sukki[d]

[a]*Faculty of Electrical Engineering, Universiti Teknologi MARA, 40450 Shah Alam, Malaysia*
[b]*Faculty of Electrical Engineering, Universiti Teknologi MARA (UiTM) Terengganu Branch, Sura Hujung 23000 Dungun, Terengganu, Malaysia*
[c]*Faculty of Electrical Engineering, Universiti Teknologi MARA (UiTM) Johor Branch, Pasir Gudang Campus, 81750 Masai, Johor, Malaysia*
[d]*School of Computing, Engineering and the Build Environment, Edinburgh Napier University, Edinburgh EH10 5DT, United Kingdom*
**Corresponding author. Tel.: 03-5544 5182; e-mail: habibahzulkefle@uitm.edu.my*

Received 15 September 2023, Revised 1 October 2025, Accepted 27 October 2025

ABSTRACT

This study addresses the underutilized potential of harvesting mechanical energy from routine human activities, while also addressing environmental and flexibility concerns associated with conventional lead-based piezoelectric materials. With the increasing demand for sustainable and eco-friendly energy solutions, lead-free piezoelectric technologies have emerged as a promising alternative, particularly in the development of flexible nanogenerators. In this study, the flexible PVDF/$BaTiO_3$ composite films fabricated via drop casting with varying $BaTiO_3$ filler loadings (1 wt%, 3 wt%, and 5 wt%) were analyzed for their influence on piezoelectric performance. Characterization techniques included contact angle analysis, FESEM, XRD, FTIR, and piezoelectric output. Results showed that 1 wt% $BaTiO_3$ yielded the highest output voltage (8.24 V), attributed to optimal β-phase formation. However, loadings beyond 3 wt% led to void formation and particle agglomeration, reducing β-phase crystallinity and overall performance. These findings demonstrate that controlled $BaTiO_3$ loading enhances piezoelectric performance while promoting environmental safety and device flexibility.

Keywords: *Lead-free piezoelectric, PVDF, β-phase formation, $BaTiO_3$, Flexible nanogenerator*

1. INTRODUCTION

The depletion and unreliability of conventional electricity generation methods have intensified the search for sustainable alternatives. Fossil fuels and nuclear power, the primary conventional energy sources, are non-renewable and will eventually be exhausted. Furthermore, the extraction and processing of fossil fuels generate significant carbon emissions, contributing to environmental degradation [1]. In recent years, the global focus on renewable energy (RE) sources has intensified due to rising concerns over environmental degradation and the depletion of fossil fuels. Renewable energy refers to energy generated from naturally replenished resources, such as solar, water, wind, biomass, and ocean-based sources like tidal and wave energy [2]. Despite their eco-friendly nature, RE sources have limitations. For example, solar and wind energy suffer from the intermittent nature of their supply [3]. Solar energy generation depends on solar irradiance, which fluctuates throughout the day and is unavailable at night, while wind power relies on wind availability, which can be irregular and inconsistent. This variability poses challenges in ensuring a consistent and reliable energy supply. Another disadvantage is the substantial land area required to harness renewable energy effectively; for instance, solar farms and wind turbines need large installations to capture sufficient energy from the sun and wind [3]. These limitations have driven research into alternative energy harvesting technologies, such as piezoelectric systems, with the objective of overcoming the drawbacks associated with conventional renewable sources.

Alternative energy harvesting technologies have emerged as practical solutions to supplement the shortcomings of renewable energy. Piezoelectric energy harvesting is a popular approach in the field of power generation. It involves generating electricity from ambient energy resources present in the environment. The demand for energy harvesting has led to an increasing investment in research and development for piezo solutions [4]. Piezoelectric nanogenerator (PENG) is a device that utilizes nanostructured piezoelectric materials to produce electric charges when subjected to mechanical stress. The most widely used piezoelectric materials are zinc oxide (ZnO), lead zirconate titanate (PZT), barium titanate (BaTiO3), sodium perborate (NaNbO3) and potassium niobate (KNbO3) [5]. The aim is to contribute to the realization of self-powered electronic devices, wearable technologies, and sensor networks that can operate autonomously, thereby reducing our dependence on conventional energy sources [6].

Recently, PZT has been a highly utilized piezoelectric material due to its exceptional piezoelectric capabilities

close to the morphotropic phase boundary between the rhombohedral and tetragonal phases [7]. The peak output voltage and output power generated from the PZT nanogenerator were 1.63V and 0.03μW with a load resistance of 6MΩ [8]. However, PZT is not environmentally sustainable as it contains lead oxide, which is poisonous. Currently, there is an increase in demand for lead-free piezoelectric materials due to growing worldwide environmental concerns. Lead-free piezoelectric materials such as $BaTiO_3$, ZnO, and $BiFeO_3$ have made a significant contribution to piezoelectric technology due to their potential for producing environmentally friendly and sustainable energy harvesting devices [9]. Other than being non-toxic, the lead-free piezoelectric is also easier to obtain and cost-effective in comparison to those containing lead [10]. The development of lead-free piezoelectric nanogenerators offers eco-friendly alternatives for powering portable electronics and reducing the dependence on conventional power sources [11].

Piezoelectric materials can be categorized as single crystals, ceramics, polymers, and composites [12]. Polyvinylidene fluoride (PVDF) is currently being investigated as an alternative piezoelectric material, as it is compatible with other piezoelectric materials. The semicrystalline polymer PVDF has five different phases (α, β, γ, δ, and ε), and among these phases, the β polymorph has high piezoelectric properties. This is due to its all trans (TTT) in a planar zigzag conformation, which makes the electroactive β polymorph most suitable for piezoelectric nanogenerator applications [13]. Besides, PVDF possesses a high piezoelectric voltage constant (g33), although it exhibits a lower dielectric constant [14]. The researchers are actively addressing the significant challenges of the low piezoelectric performance of PVDF nanogenerator films. There are different ways to increase the electroactive β-phase fraction (piezoelectric properties) in a polymer filler composite, such as using of external electric poling process, stretching, and filler loading [15]. Among these techniques, the impregnation of nanofillers having inherent high piezoelectric properties [16].

Commonly utilized ceramic nanofillers with polymer piezoelectric characteristics include zinc oxide (ZnO), lead zirconate titanate (PZT), barium titanate (BT), and potassium sodium niobate (KNN). However, achieving the desired performance of piezoelectric ceramics remains challenging [17]. Many researchers have fabricated PVDF composites with nanofillers such as BT and ZnO to produce composite nanogenerators. The morphology, structure, and characteristics of electrospun BT and ZnO nanofibers are greatly influenced by the experimental conditions and the properties of the precursor materials [18]. Barium titanate ($BaTiO_3$) ceramics are considered among the most promising electroceramic materials. Therefore, this study focuses on optimizing the loading percentage of $BaTiO_3$ in PVDF to enhance the piezoelectric performance of PVDF nanogenerator films. The structural and piezoelectric properties of the deposited PVDF/$BaTiO_3$ films are systematically studied via contact angle measurements, Field-Emission Scanning Electron Microscopy (FESEM), X-ray diffraction (XRD), Fourier Transform Infrared spectroscopy (FTIR), and piezoelectric response testing.

2. METHODOLOGY

The methodology employed in this study investigates the influence of $BaTiO_3$ weight percentages on the structural and electrical properties of PVDF/$BaTiO_3$ nanogenerator films. Fig. 1 shows the fabrication process involved in preparing PVDF/$BaTiO_3$ films, where it starts with film deposition using the drop-casting method, followed by an annealing process, and lastly the film's characterization. The characterization techniques include contact angle measurements, Field-Emission Scanning Electron Microscopy (FESEM), X-Ray Diffraction (XRD), Fourier Transform Infrared Spectroscopy (FTIR), and piezoelectric response testing. Finally, the results are analyzed to determine the optimized $BaTiO_3$ loading percentage and evaluate the effect of filler loading on the electrical and structural properties.

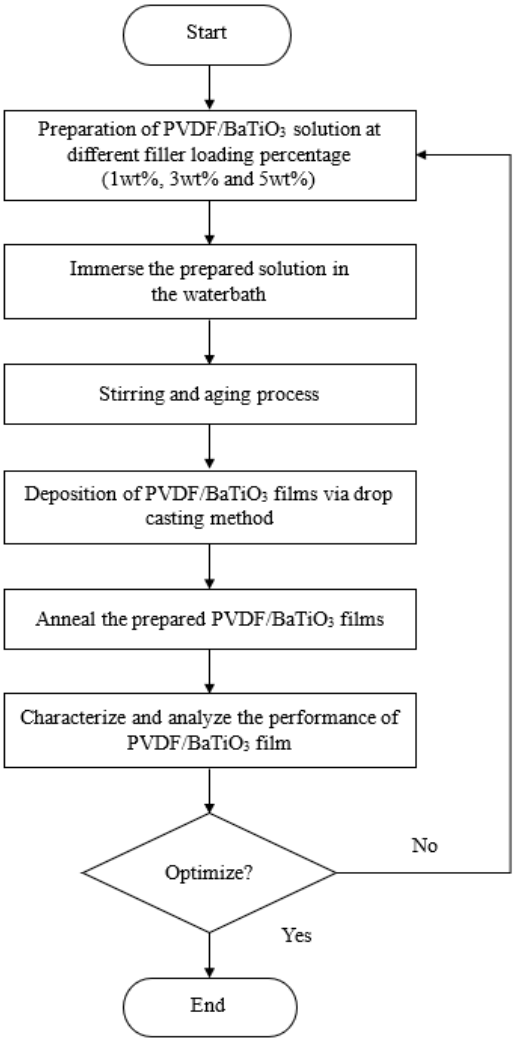

Figure 1. The Overall Process of Deposition of PVDF/BaTiO3 Nanogenerator Films.

2.1. PVDF/$BaTiO_3$ Film Preparation

The PVDF was dissolved in the polar solvent N, N-Dimethylformamide (DMF) at a concentration of 30g/L. The $BaTiO_3$ nanopowder [19] was poured into the PVDF solution by using different loading percentages (1wt.%, 3wt.% and 5wt.%). The solution was then immersed in a water bath for 1 hour at a temperature of 70°C. Next, the prepared solution underwent a stirring and aging process for 48 hours using a magnetic stirrer at 750 rpm, maintaining a temperature of 70°C. The prepared solution was poured into the petri dish using the drop-casting method. The solution volume for all samples was fixed at 2.5 mL to ensure even distribution and minimize thickness irregularities. The solution was then put into an oven for the annealing process at 120°C for 90 minutes. After the annealing process, the film was left to cool off before undergoing the peeling process.

2.2. PVDF/$BaTiO_3$ Film Characterization

The deposited PVDF/$BaTiO_3$ nanogenerator film was inspected on its wettability using a water surface analysis system (Contact Angle - AST Products, Inc. VCA 3000s) to identify the hydrophilic or hydrophobic characteristics. Field Emission Scanning Electron Microscopy (FESEM) analysis allows for the investigation of surface morphology. Prior to the FESEM characterization, the platinum (Pt) coatings were applied to the samples to reduce charging in the FESEM observation. Fourier Transform Infrared Spectroscopy (FTIR- PerkinElmer Spectrum One) and X-ray Diffraction (XRD- RIGAKU D/MAX-2200/PC) provide information on the material structure to distinguish between different crystalline forms.

The piezoelectric performance of the PVDF/$BaTiO_3$ films was evaluated by measuring the output voltage generated under mechanical stress. Prior to the investigation, the film was cut into an area (2.0 x 1.5) cm^2 and stacked between copper electrodes as shown in Fig. 2. Two jumper wires were connected to both ends of the copper before connecting with the oscilloscope in nanogenerator fabrication. The piezoelectric response was measured using a tapping process with a solenoid tapper, applying a mechanical force of 2 N-m at a frequency of 10 Hz, as shown in Fig. 3. The waveforms of the open circuit peak-to-peak output voltages were then observed.

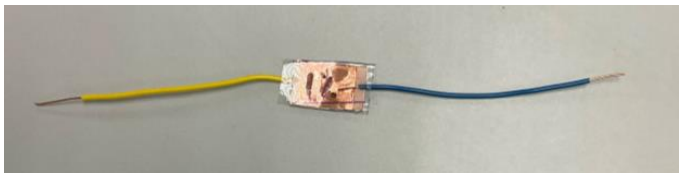

Figure 2. Fabricated PVDF/BaTiO3 Nanogenerator Film.

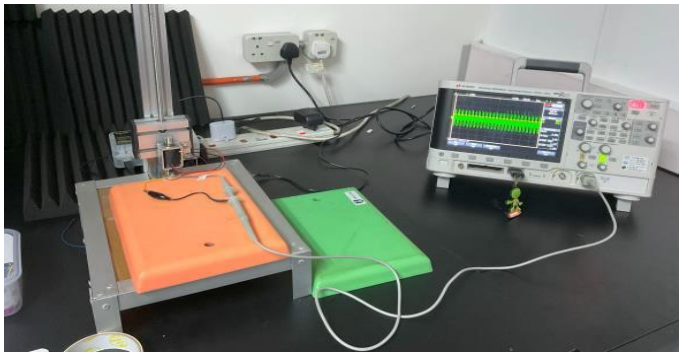

Figure 3. Experimental Setup of Piezo Response Analysis.

3. RESULTS AND DISCUSSIONS

The surface morphology of PVDF/$BaTiO_3$ films was examined using FESEM analysis, as shown in Fig. 4. The aim of this examination is to investigate and understand the effect of $BaTiO_3$ filler addition on the surface morphology of PVDF/$BaTiO_3$ films. The investigation of the films was conducted at a magnification of 50,000x. $BaTiO_3$ nanoparticles act as heterogeneous nucleation sites within the PVDF matrix.

PVDF is well-known for its semi-crystalline nature, characterized by the formation of spherulites shown in Fig. 4(a) during the crystallization process. When the $BaTiO_3$ fillers were introduced into the PVDF matrix (1wt%), significant changes occurred in the microstructure, particularly destructing the structure of PVDF spherulitic morphology. Based on the FESEM analysis, the PVDF/BaTiO3 film with 1wt% $BaTiO_3$ (Fig. 4b) demonstrated the most favourable morphology among the tested weight percentages. The film exhibited a well-defined and uniform surface morphology with evenly dispersed $BaTiO_3$ particles. The 1wt% PVDF/$BaTiO_3$ film showed minimal agglomeration and voids compared to other weight percentages.

As the concentration of $BaTiO_3$ increases above 1wt%, this disruption becomes more pronounced. There is an observable trend indicating that $BaTiO_3$ begins to dominate the PVDF matrix. This can be observed through the presence of voids as shown in Fig. 4(c). Voids formation happens when inadequate dispersion of $BaTiO_3$ nanoparticles in the film. With further increases in the dopant percentage, there is a high tendency for $BaTiO_3$ nanoparticles to agglomerate, as shown in Fig. 4(d). The nanocomposite film with a defect or void can be observed in the image, demonstrating the agglomeration of the nanocomposite film [20].

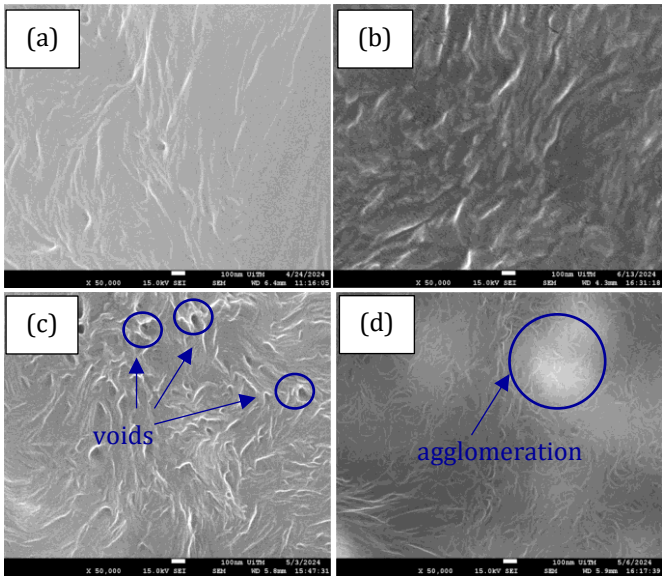

Figure 4. FESEM Images of (a) Undoped, (b) 1wt%, (c) 3wt%, (d) 5wt% PVDF/BaTiO3 Nanogenerator Films.

The XRD analysis was conducted to determine the crystallinity of the film. Fig. 5 presents prominent peaks at 2θ=20.06° (200), which confirms the presence of the β-phase of pure PVDF [21]. Fig. 5 shows the XRD spectra of undoped and PVDF/$BaTiO_3$ nanogenerator films at different weight percentages. Addition of $BaTiO_3$ causes the crystallinity peak associated to PVDF demolished (Fig. 6). The XRD spectra of PVDF/$BaTiO_3$ films revealed a polycrystalline phase with eight diffraction peaks at [22.12° (100), 31.44° (101), 38.84° (111), 45.22° (200), 51.10° (201), 56.24° (211), 66.00° (202), and 75.38° (310)] which matched with JCPDS Card No. 05-0626 [22], [23].

Strong and narrow diffraction peaks indicate a highly crystalline film, while the absence of additional signals indicates the prepared films were devoid of contaminants. Interestingly, the results show that a higher filler percentage improves the crystallinity of the PVDF/$BaTiO_3$ films, in which at the lowest weight percentage (1 wt%), the intensity of the diffraction is lower compared to the highest weight percentage (5wt%). This is because the amount of $BaTiO_3$ acts as nucleation sites to improve the film's crystallinity. Besides, the results indicate that the $BaTiO_3$ added into the PVDF matrix was polycrystalline, and the insignificant change in the XRD spectra confirmed the successful incorporation of $BaTiO_3$ into the matrix.

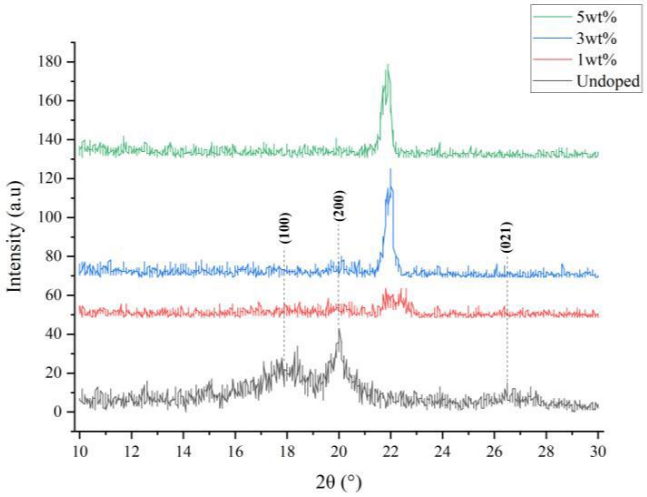

Figure 5. X-ray Diffraction Patterns at 2θ of 10°-20°.

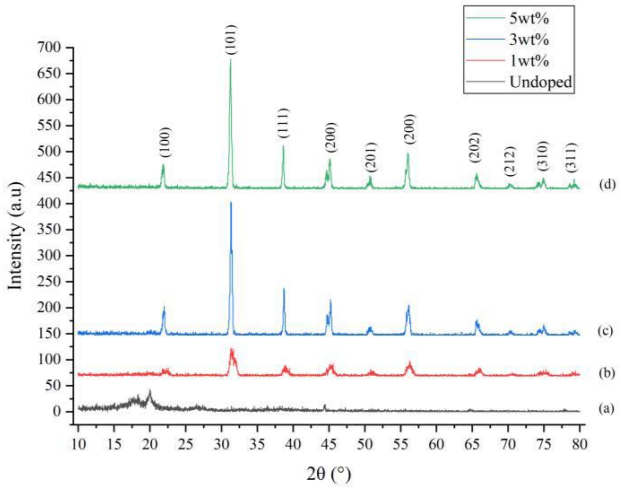

Figure 6. X-ray Spectra of (a) undoped, (b) 1wt%, (c) 3wt%, (d) 5wt% PVDF/BaTiO3 Nanogenerator Films.

The FTIR spectra for PVDF/$BaTiO_3$ nanogenerator films with different $BaTiO_3$ weight percentages (1wt%, 3wt%, and 5wt%) are shown in Fig. 7. The spectra reveal that all samples contain the semicrystalline polymer PVDF, exhibiting the formation of all polymorph phases (α, β, and γ). The FTIR spectra reveal the peaks of the α non-polar phase of PVDF, with IR bands located at 532 cm^{-1}, 762 cm^{-1}, and 975 cm^{-1}, are nearly entirely diminished in the 1wt%, 3wt%, and 5wt% samples in comparison to the undoped sample. Additionally, the absorption band located at 840 cm^{-1}, 856 cm^{-1}, 1170 cm^{-1}, and 1400 cm^{-1} shows a prominent peak, which indicates β-phase.

It can be observed that the absorption band for all polymorph peaks was improved significantly as the $BaTiO_3$ filler was added to the PVDF film (1wt %). A sharp and well-resolved band at 840 cm^{-1} indicates the β-phase, whereas a broad band corresponds to the γ-phase. The FTIR spectra for the 1 wt% PVDF/$BaTiO_3$ film show a greater presence of the β-phase; however, further increases in $BaTiO_3$ weight percentage result in narrower absorption peaks, indicating lower β-phase content. This proves that the addition of 1 wt% $BaTiO_3$ filler acts as nucleation sites to promote β-phase crystallization. However, when the filler loading exceeds 1 wt%, the overall β-phase content is significantly reduced, suggesting that the aligned chains become disrupted. This reduction is attributed to agglomeration within the film, which creates mechanical defects and stress concentrations that hinder uniform chain alignment. This finding is in line with work done by Kabir et al., who noticed a significant decrease in the intensity of the absorption peak as the $BaTiO_3$ concentration increased [24]. In addition, the FTIR analysis suggests that, although the addition of filler can help in an improvement in the β-phase of PVDF/$BaTiO_3$ film, there is a threshold weight percentage of $BaTiO_3$ loading. A higher amount of filler loading negatively affected the overall crystalline nature of PVDF and resulted in the formation of more amorphous structures.

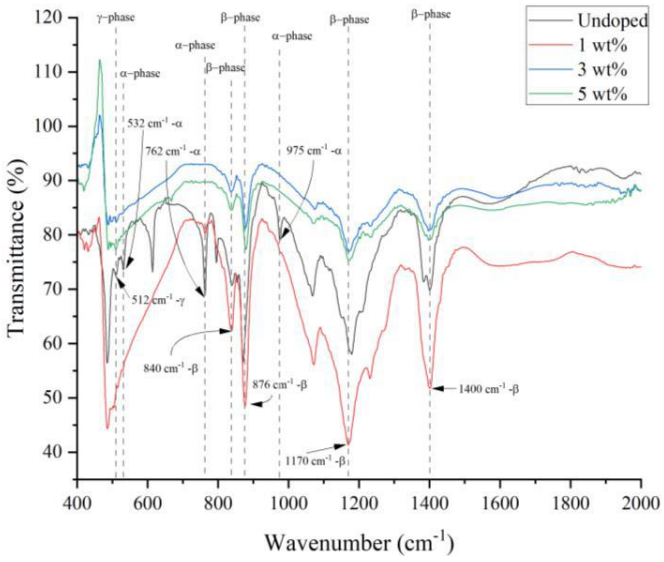

Figure 7. FTIR Spectra for PVDF/BaTiO3 Nanogenerator Films.

As seen from the XRD and FTIR analyses, XRD showed an improvement in crystallinity at higher filler percentages, while FTIR analysis revealed a reduction in β-phase content at higher loadings. This is because XRD and FTIR probe different aspects of the composite. The apparent increase in crystallinity observed in the XRD analysis at higher $BaTiO_3$ weight percentages is attributed to the intrinsic crystallinity of $BaTiO_3$ itself and the overall increase in the ordered content of the PVDF/$BaTiO_3$ composite. In contrast, FTIR focuses on PVDF polymorphs and shows that the electroactive β-phase fraction within the polymer decreases once the filler exceeds the optimal loading (>1 wt%). Above this threshold, particle agglomeration and reduced chain mobility favor α-phase nucleation and dilute the PVDF contribution, lowering the relative β-phase content even though the total crystallinity of the PVDF/$BaTiO_3$ composite increases. Thus, total crystallinity can rise while the PVDF β-phase fraction decreases.

In contact angle analysis, the image of the angle between the water droplet and PVDF/$BaTiO_3$ film was recorded as shown in Fig. 8. The analysis of the contact angle of PVDF/$BaTiO_3$ film provided significant insight into its surface characteristics and wettability behaviour. The contact angles that were measured were constantly larger than 90° as tabulated in Table I. A film's surface is considered hydrophilic if the contact angle is less than 90°, while considered hydrophobic if the contact angle is greater than 90° [25]. This indicates that the film's surface exhibited a significant hydrophobicity or resistance to being wetted by water. In addition, when $BaTiO_3$ filler is first introduced into the PVDF polymer matrix at 1wt%, there is a slight reduction in the contact angle from 95.50° to 91.40°.

Figure 8. The Angle Between the Water Droplet and the Deposited Film Surface.

Table 1 Voltage Peak to Peak and Contact Angle of PVDF/$BaTiO_3$ Nanogenerator Films

Weight Percentage of BaTiO3 (wt%)	Open Circuit Voltage, Vpp (V)	Contact Angle (°)
0	5.4	95.50
1	8.24	91.40
3	5.95	90.30
5	3.07	90.00

Hydrophobic surfaces are highly beneficial for piezoelectric materials, as they improve electrical insulation by reducing the risk of leakage currents that can occur when water is adsorbed onto the surface. This benefit is vital for the performance of piezoelectric devices across a wide range of applications, such as wearable electronics and biomedical devices. In the context of these applications, the hydrophobicity of the film plays a significant role in device durability and stability. A hydrophobic surface limits water absorption and prevents hydrolytic degradation to ensure consistent electrical and mechanical properties even under prolonged exposure to sweat, humidity, and biological fluids. Therefore, optimization of $BaTiO_3$ filler into PVDF is essential to balance hydrophobicity-driven environmental stability, piezoelectricity sensitivity, and mechanical durability for reliable sensor and biomedical sensor performance.

In addition, Table 1 tabulates the open circuit voltage, while Fig. 9 shows the output waveform of the PVDF/ $BaTiO_3$ films. Based on the figure, the undoped PVDF film generated a small open circuit voltage of 5.4 Vpp. Interestingly, as the BaTiO3 was added to the PVDF film (1wt%), the Vpp value was significantly increased to 8.24V. This is due to the enhancement of the β-phase in the film, as confirmed by the FTIR analysis shown in Fig. 7. Theoretically, the β-phase is responsible for the electroactive properties [26] and is the most polar crystalline phase in PVDF. All-trans chain conformation in this phase produced the strongest net dipole moment along the polymer chains. Thus, the enhancement of the β-phase leads to a higher piezoelectric coefficient and results in better output voltage.

As the weight percentage of $BaTiO_3$ increased to 3wt% and 5wt%, the open circuit voltage exhibited a decrease compared to the 1wt% doped film, as shown in Fig. 10. This reduction in open circuit voltage shows that the piezoelectric performance becomes disrupted at higher

weight percentage of $BaTiO_3$. This might be due to the formation of voids and agglomeration of the particles, which leads to non-uniform dispersion and finally reduces the β-phase formation. This is proven by FESEM images shown in Fig. 4(c and d) that show the presence of voids and agglomeration in the surface morphology of PVDF/ $BaTiO_3$ films. The voids and agglomeration observed in these films disturbed uniform chain alignment in these films due to mechanical defects and stress concentrations. This finding indicates that 1 1wt% of $BaTiO_3$ provides the optimal conditions for maximizing the piezoelectric response of the PVDF/ $BaTiO_3$ film.

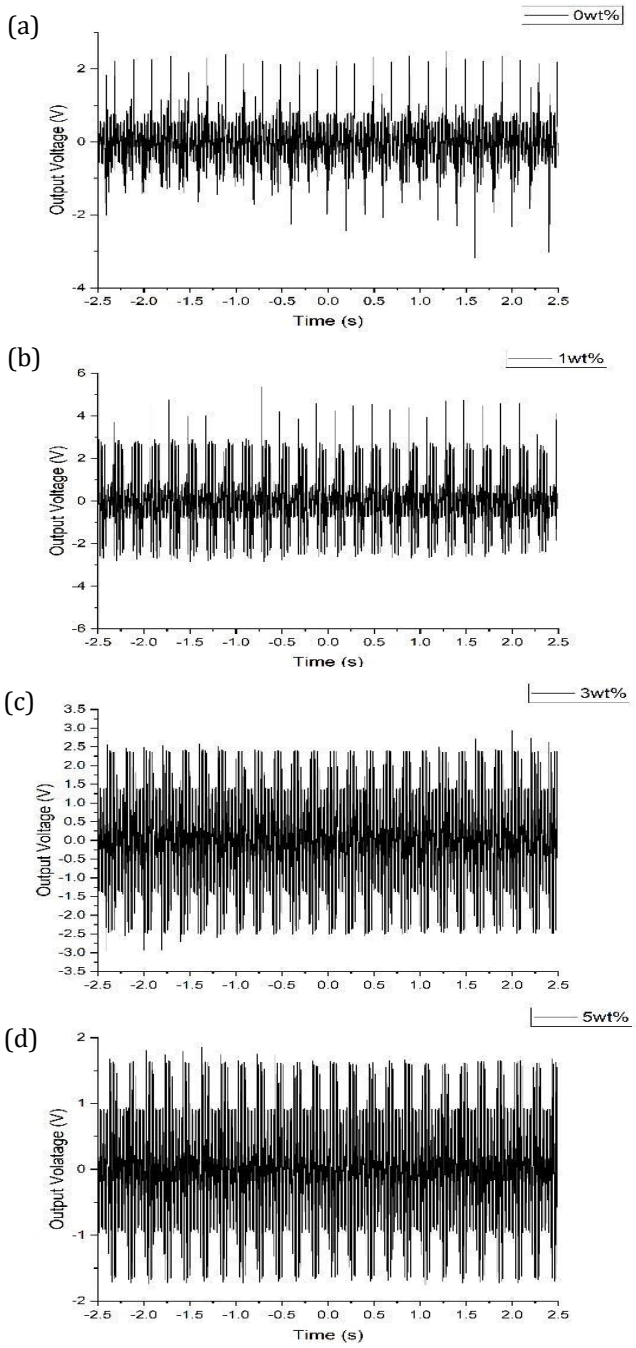

Figure 9. Open Circuit Voltage of (a) Undoped, (b) 1wt%, (c) 3wt%, (d) 5wt% PVDF/$BaTiO_3$ Nanogenerator Films.

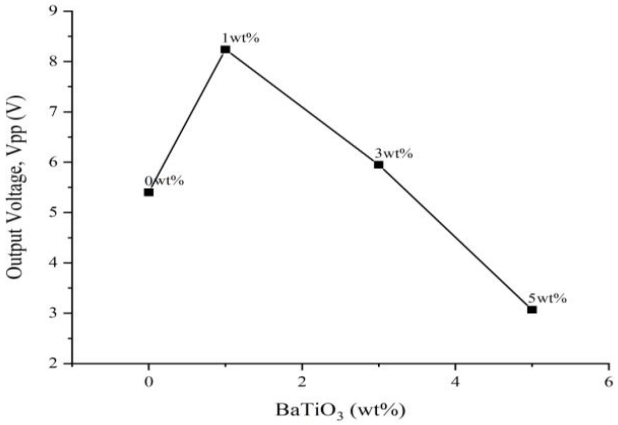

Figure 10. Output Voltage of PVDF/$BaTiO_3$ Nanogenerator Films.

4. CONCLUSION

This study highlights the significant impact of $BaTiO_3$ loading percentage (1wt%, 3wt% and 5wt%) on the performance of the flexible PVDF nanogenerator films. The film's performance was investigated through several characterizations using contact angle, FESEM, XRD, FTIR, and piezoelectric response analyses. In terms of surface morphology, FESEM analysis revealed that the 1wt% of $BaTiO_3$ film exhibited a well-dispersed and uniform surface with minimal agglomeration and voids. Higher filler loadings, however, resulted in voids and agglomerates, disrupting the film's compactness. The study concludes the optimal $BaTiO_3$ content is 1wt% in the PVDF matrix, as the film achieved the highest open circuit output voltage of 8.24 Vpp under 2Nm mechanical stress. This is contributed from the enhancement of β-phase produced in 1wt% film in which $BaTiO_3$ acts as a nucleating agent, guiding the PVDF chain to align in β-phase orientation. The wettability analysis demonstrated that all prepared films' surfaces exhibited hydrophobicity, which could improve the durability of the device. Overall, these findings provide valuable insights into the deposition and optimization of PVDF/$BaTiO_3$ nanogenerator films, emphasizing the importance of controlled BaTiO3 content to maximize the piezoelectric performance.

ACKNOWLEDGMENTS

The authors extend their gratitude to Universiti Teknologi MARA (UiTM) for providing funding. The authors would also like to thank the Nano-Electronics Centre (NET), Faculty of Electrical Engineering, UiTM, and the Faculty of Chemical Engineering, UiTM, for providing the laboratory facilities throughout this study.

REFERENCES

[1] S. Kılıç Depren, M. T. Kartal, N. Çoban Çelikdemir, and Ö. Depren, "Energy consumption and environmental degradation nexus: A systematic review and meta-analysis of fossil fuel and renewable energy consumption," *Ecol Inform*, vol. 70, no. June, 2022, doi: 10.1016/j.ecoinf.2022.101747.

[2] C. Bou-Mosleh, P. Rahme, P. Beaino, R. Mattar, and E. A. Nassif, "Contribution to clean energy production using a novel wave energy converter: Renewable energy," *2014 International Conference on Renewable Energies for Developing Countries, REDEC 2014*, pp. 108–111, 2014, doi: 10.1109/REDEC.2014.7038540.

[3] L. Lakatos, G. Hevessy, and J. Kovács, "Advantages and disadvantages of solar energy and wind-power utilization," *World Futures: Journal of General Evolution*, vol. 67, no. 6, pp. 395–408, 2011, doi: 10.1080/02604020903021776.

[4] T. Vithusan, M. N. F. Nashira, and S. U. Adikary, "Modelling and Simulation of a Vertically Integrated Zinc Oxide Piezoelectric Nanogenerator," *MERCon 2022 - Moratuwa Engineering Research Conference, Proceedings*, pp. 1–6, 2022, doi: 10.1109/MERCon55799.2022.9906201.

[5] A. Bouhamed, Q. Binyu, and O. Kanoun, "Flexible lead-free piezoelectric polymer composite nanogenerator with enhanced crystallinity," *Proceedings of the 17th International Multi-Conference on Systems, Signals and Devices, SSD 2020*, pp. 130–134, 2020, doi: 10.1109/SSD49366.2020.9364101.

[6] S. Bairagi, Shahid-ul-Islam, M. Shahadat, D. M. Mulvihill, and W. Ali, "Mechanical energy harvesting and self-powered electronic applications of textile-based piezoelectric nanogenerators: A systematic review," *Nano Energy*, vol. 111, no. March, p. 108414, 2023, doi: 10.1016/j.nanoen.2023.108414.

[7] S. Missaoui, A. Bouhamed, H. Nouri, N. Abdelmoulah, H. Khemakham, and O. Kanoun, "Lead-Free Ba0.85Ca0.15Zr0.1Ti0.1O3for High Piezoelectric Performance Flexible Nanogenerator," *Proceedings of International Workshop on Impedance Spectroscopy, IWIS 2021*, pp. 30–32, 2021, doi: 10.1109/IWIS54661.2021.9711813.

[8] X. Chen, S. Xu, N. Yao, and Y. Shi, "1.6 v nanogenerator for mechanical energy harvesting using PZT nanofibers," *Nano Lett*, vol. 10, no. 6, pp. 2133–2137, 2010, doi: 10.1021/nl100812k.

[9] S. Veeralingam, O. P. Nanda, and S. Badhulika, "Lead-free Bi2CuO4 interspersed into PDMS matrix-based bifunctional piezoelectric nanogenerator for vibrational energy harvesting and visible light photodetection applications," *J Alloys Compd*, vol. 961, p. 171127, 2023, doi: 10.1016/j.jallcom.2023.171127.

[10] H. Wei *et al.*, "An overview of lead-free piezoelectric materials and devices," *J Mater Chem C Mater*, vol. 6, no. 46, pp. 12446–12467, 2018, doi: 10.1039/c8tc04515a.

[11] X. Wang, "Piezoelectric nanogenerators-Harvesting ambient mechanical energy at the nanometer scale," *Nano Energy*, vol. 1, no. 1, pp. 13–24, 2012, doi: 10.1016/j.nanoen.2011.09.001.

[12] S. Bairagi and S. W. Ali, "Poly (vinylidine fluoride) (PVDF)/Potassium Sodium Niobate (KNN) nanorods based flexible nanocomposite film: Influence of KNN concentration in the performance of nanogenerator," *Org Electron*, vol. 78, no. November 2019, p. 105547, 2020, doi: 10.1016/j.orgel.2019.105547.

[13] E. Kar, N. Bose, B. Dutta, S. Banerjee, N. Mukherjee, and S. Mukherjee, "2D SnO2 nanosheet/PVDF composite based flexible, self-cleaning piezoelectric energy harvester," *Energy Convers Manag*, vol. 184, no. January, pp. 600–608, 2019, doi: 10.1016/j.enconman.2019.01.073.

[14] S. Mishra, L. Unnikrishnan, S. K. Nayak, and S. Mohanty, "Advances in Piezoelectric Polymer Composites for Energy Harvesting Applications: A Systematic Review," *Macromol Mater Eng*, vol. 304, no. 1, pp. 1–27, 2019, doi: 10.1002/mame.201800463.

[15] N. Soin *et al.*, "High performance triboelectric nanogenerators based on phase-inversion piezoelectric membranes of poly(vinylidene fluoride)-zinc stannate (PVDF-ZnSnO3) and polyamide-6 (PA6)," *Nano Energy*, vol. 30, no. October, pp. 470–480, 2016, doi: 10.1016/j.nanoen.2016.10.040.

[16] U. Yaqoob, A. S. M. I. Uddin, and G. S. Chung, "A novel tri-layer flexible piezoelectric nanogenerator based on surface- modified graphene and PVDF-BaTiO 3 nanocomposites," *Appl Surf Sci*, vol. 405, pp. 420–426, 2017, doi: 10.1016/j.apsusc.2017.01.314.

[17] C. Zhao, J. Niu, Y. Zhang, C. Li, and P. Hu, "Coaxially aligned MWCNTs improve performance of electrospun P(VDF-TrFE)-based fibrous membrane applied in wearable piezoelectric nanogenerator," *Compos B Eng*, vol. 178, no. September, p. 107447, 2019, doi: 10.1016/j.compositesb.2019.107447.

[18] R. S. Sabry and A. D. Hussein, "PVDF: ZnO/BaTiO3 as high out-put piezoelectric nanogenerator," *Polym Test*, vol. 79, no. July, 2019, doi: 10.1016/j.polymertesting.2019.106001.

[19] A. A. M. Noordin, A. A. Aziz, N. Khairuddin, and N. Burham, "The Effect of Calcination Temperature on the Structural Properties of BaTiO3 and (Ba0.85Ca0.15)(Zr0.1Ti0.9)O3 Using the SSR Method," *Materials Science Forum*, vol. 1055 MSF, pp. 87–92, 2022, doi: 10.4028/p-22p8w2.

[20] M. Kumar, N. D. Kulkarni, and P. Kumari, "Piezoelectric performance enhancement of electrospun functionally graded PVDF/BaTiO3 based flexible nanogenerators," *Mater Res Bull*, vol. 174, no. November 2022, p. 112739, 2024, doi: 10.1016/j.materresbull.2024.112739.

[21] P. Martins, A. C. Lopes, and S. Lanceros-Mendez, "Electroactive phases of poly(vinylidene fluoride): Determination, processing and applications," *Prog Polym Sci*, vol. 39, no. 4, pp. 683–706, 2014, doi: 10.1016/j.progpolymsci.2013.07.006.

[22] Y. Yao *et al.*, "Piezoelectric BaTiO3 with the milling treatment for highly efficient piezocatalysis under vibration," *J Alloys Compd*, vol. 905, p. 164234, 2022, doi: 10.1016/j.jallcom.2022.164234.

[23] L. Wang *et al.*, "Ferroelectric BaTiO3@ZnO heterostructure nanofibers with enhanced pyroelectrically-driven-catalysis," *Ceram Int*, vol. 45, no. 1, pp. 90–95, 2019, doi: 10.1016/j.ceramint.2018.09.137.

[24] H. Kabir, H. Kamali Dehghan, S. Mashayekhan, R. Bagherzadeh, and M. S. Sorayani Bafqi, "Hybrid fibrous (PVDF-BaTiO3)/ PA-11 piezoelectric patch as an energy harvester for pacemakers," *Journal of Industrial Textiles*, vol. 51, no. 3_suppl, pp. 4698S-4719S, 2022, doi: 10.1177/15280837211057575.

[25] R. Moradi, J. Karimi-Sabet, M. Shariaty-Niassar, and M. A. Koochaki, "Preparation and characterization of polyvinylidene fluoride/graphene superhydrophobic fibrous films," *Polymers (Basel)*, vol. 7, no. 8, pp. 1444–1463, 2015, doi: 10.3390/polym7081444.

[26] S. Mahboubizadeh, S. T. Dilamani, and S. Baghshahi, "Piezoelectricity performance and β-phase analysis of PVDF composite fibers with BaTiO3 and PZT reinforcement," *Heliyon*, vol. 10, no. 3, p. e25021, 2024, doi: 10.1016/j.heliyon.2024.e25021.